POTSDAM-INSTITUT FÜR
KLIMAFOLGENFORSCHUNG

Originally published as:

Future sea level rise constrained by observations and long-term commitment

Matthias Mengel[a,b], Anders Levermann[a,b,c,1], Katja Frieler[a], Alexander Robinson[a,d,e], Ben Marzeion[f], and Ricarda Winkelmann[a,b]

[a]Potsdam Institute for Climate Impact Research, 14473 Potsdam, Germany; [b]Physics Institute, Potsdam University, 14476 Potsdam, Germany; [c]Lamont-Doherty Earth Observatory, Columbia University, Palisades, NY 10964; [d]Universidad Complutense de Madrid, 28040 Madrid, Spain; [e]Instituto de Geociencias (IGEO), Consejo Superior de Investigaciones Científicas - Universidad Complutense de Madrid, 28040 Madrid, Spain; and [f]Institute of Geography, University of Bremen, 28359 Bremen, Germany

Sea level has been steadily rising over the past century, predominantly due to anthropogenic climate change. The rate of sea level rise will keep increasing with continued global warming, and, even if temperatures are stabilized through the phasing out of greenhouse gas emissions, sea level is still expected to rise for centuries. This will affect coastal areas worldwide, and robust projections are needed to assess mitigation options and guide adaptation measures. Here we combine the equilibrium response of the main sea level rise contributions with their last century's observed contribution to constrain projections of future sea level rise. Our model is calibrated to a set of observations for each contribution, and the observational and climate uncertainties are combined to produce uncertainty ranges for 21st century sea level rise. We project anthropogenic sea level rise of 28–56 cm, 37–77 cm, and 57–131 cm in 2100 for the greenhouse gas concentration scenarios RCP26, RCP45, and RCP85, respectively. Our uncertainty ranges for total sea level rise overlap with the process-based estimates of the Intergovernmental Panel on Climate Change. The "constrained extrapolation" approach generalizes earlier global semiempirical models and may therefore lead to a better understanding of the discrepancies with process-based projections.

sea level rise | climate change | climate impacts

Sea level has been rising between 16 and 19 cm since 1900 (1, 2) with a rate of around 3 cm per decade since 1990 (3, 4). Thermal expansion of the oceans and retreating glaciers are the main contributors to sea level rise in the past century and the near future. On multicentennial timescales, the Greenland and Antarctic ice sheets will likely dominate global sea level rise (5). Future sea level rise will pose challenges to coastal regions around the globe, and robust projections are needed to guide adaptation investment and provide incentives for climate mitigation (6).

Projecting sea level relies on the understanding of the processes that drive sea level changes and on reliable data to verify and calibrate models. So-called process-based models now deliver projections for the main components of climate-driven sea level rise—thermal expansion, glaciers and ice caps, the Greenland ice sheet, and the Antarctic ice sheet—although solid ice discharge (SID) from the ice sheets is still difficult to constrain (3). Semiempirical models follow a different approach and use the statistical relation between global mean temperature (7, 8) or radiative forcing (9, 10) and sea level from past observations. Without aiming to capture the full physics of the sea level components, they project future sea level assuming that the past statistical relation also holds in the future. Their simpler nature makes them feasible for probabilistic assessments and makes their results easier to reproduce.

The long-term multicentennial to millennial sensitivity of the main individual sea level contributors to global temperature changes can be constrained by paleoclimatic data and is more easily computed with currently available process-based large-scale models than are decadal to centennial variations (5, 11). In addition, there is an increasing number of observations available for the historical

individual contributions to sea level rise, which capture the early response to global temperature changes.

Here we seek to combine the long-term sensitivity (or long-term commitment) and the individual observations to constrain estimates of near-future sea level rise by semiempirical relations for each sea level contributor. This expands the classical semiempirical approach that has so far been based on total sea level rise. We use a pursuit curve to estimate sea level rise in accordance with the respective long-term sensitivity. We define $S(t)$ as the time-dependent sea level contribution, $S_{eq}(T, \alpha)$ is the long-term sensitivity for the sea level component as a function of global mean temperature T and the commitment factor α (see methods), and τ is the response timescale. We can then model the short-term rate of sea level rise as a function of global mean temperature as

$$\frac{dS}{dt} = \frac{S_{eq}(T(t), \alpha) - S(t)}{\tau}. \quad [1]$$

This ordinary differential equation describes a physical system in which S seeks to approach its equilibrium value (here S_{eq}) with speed linearly dependent on the deviation from the equilibrium and the inverse of τ. The approach has already been applied to project total sea level rise (10). The integrated equation yields the sea level evolution. Uncertainty in the long-term sensitivity S_{eq} is covered by variation of commitment parameters. We calibrate τ

Significance

Anthropogenic sea level rise poses challenges to coastal areas worldwide, and robust projections are needed to assess mitigation options and guide adaptation measures. Here we present an approach that combines information about the equilibrium sea level response to global warming and last century's observed contribution from the individual components to constrain projections for this century. This "constrained extrapolation" overcomes limitations of earlier global semiempirical estimates because long-term changes in the partitioning of total sea level rise are accounted for. While applying semiempirical methodology, our method yields sea level projections that overlap with the process-based estimates of the Intergovernmental Panel on Climate Change. The method can thus lead to a better understanding of the gap between process-based and global semiempirical approaches.

ENVIRONMENTAL SCIENCES

SUSTAINABILITY SCIENCE

by minimizing the sum of the squared residuals ("least-squares") between observed and modeled sea level evolution for the past for each contributor and each observational dataset.

Results

Thermal Expansion. Past thermosteric sea level rise can be inferred from observations of ocean temperature that are available for several ocean depth ranges (Fig. S1). The upper ocean layer (0–700 m) is best observed (12–14). Fewer observations are available for the middepth (14) and abyssal ocean (15). To encompass the uncertainty from the different observational datasets, we create all possible combinations of the observations from different depths to yield 12 estimates for total thermosteric sea level rise (see *Supporting Information* for details). For the given range of commitment factors, our calibration method yields equilibration times τ between 82 and 1,290 y (Table S1). Driven by observed global mean temperature change (16), our model can reproduce the different time series of observed thermosteric sea level rise (see Fig. 1*A* for a subset and Fig. S2 for the full set). The estimates for the full time period since 1900 encompass the Coupled Model Intercomparison Project Phase 5 (CMIP5) model mean (3) (Fig. 1*A*, gray lines).

With the 12 calibrated tuples of α and τ, we project the sea level contribution from thermal expansion within the 21st century for the three representative concentration pathways RCP26, RCP45, and RCP85 (17). Fig. 2*A* shows the median and very likely (5–95%) uncertainty range for the three RCP scenarios. In 2100, the thermosteric median sea level contribution is estimated to be 15 cm, 19 cm, and 29 cm for RCP26, RCP45, and RCP85, respectively (Table 1 and Fig. 2*A*). The mean sea level rise 2081–2100 compared with the 1986–2005 mean (Table S2) is close the Intergovernmental Panel on Climate Change (IPCC) projections for the three scenarios (Fig. 2*A*, bars at the right). In our probabilistic approach, the ocean heat uptake does not influence global mean temperature evolution, as opposed to the coupled IPCC simulations. This leads to higher uncertainty ranges for each scenario compared with the IPCC.

Mountain Glaciers. Global glacier volumes decline since the 19th century. Observation-based estimates of glacier mass changes (18–20) (see *Supporting Information* for description) have recently become more consistent despite their different reconstruction techniques (21). Although human influence dominated glacier loss in the second half of the 20th century, earlier retreat was mainly driven by natural climate variability and ongoing adjustment to past climate change. Glacier volumes decreased particularly fast in the Arctic (20) during a period of early warming (22) in the late 19th century and first half of the 20th century.

The human-induced part of total glacier loss increased over time and reached about 70% in recent years (23). We calibrate our semiempirical model to each of the anthropogenic parts of the observational datasets with each of the equilibrium sensitivities (see *Materials and Methods*). The 57 corresponding calibrated response times τ range from 98 y to 295 y. The observed anthropogenic sea level rise from glaciers is well reproduced for the second half of the 20th century, whereas the signal of early Arctic warming is not fully captured (Fig. 1*B* and Fig. S3). Differences remain in the early part of the time series because attribution of early Arctic warming is imperfect when the anthropogenic signal is still small.

We project a median sea level contribution of 8 cm, 9 cm, and 11 cm until 2100 for the RCP26, RCP45, and RCP85 scenarios, respectively (Fig. 2*B*). The glacier mass loss is less scenario-dependent than other contributions, and the 2081–2100 mean lies below the IPCC estimates (Fig. 2*B*, bars at the right). This is partly due to the form of its long-term contribution, which approaches a temperature-independent asymptote for strong global warming (see Fig. S4), reflecting the limited volume of the world's glaciers. The full effect of the limited global glacier mass will become apparent in the past-2100 contribution.
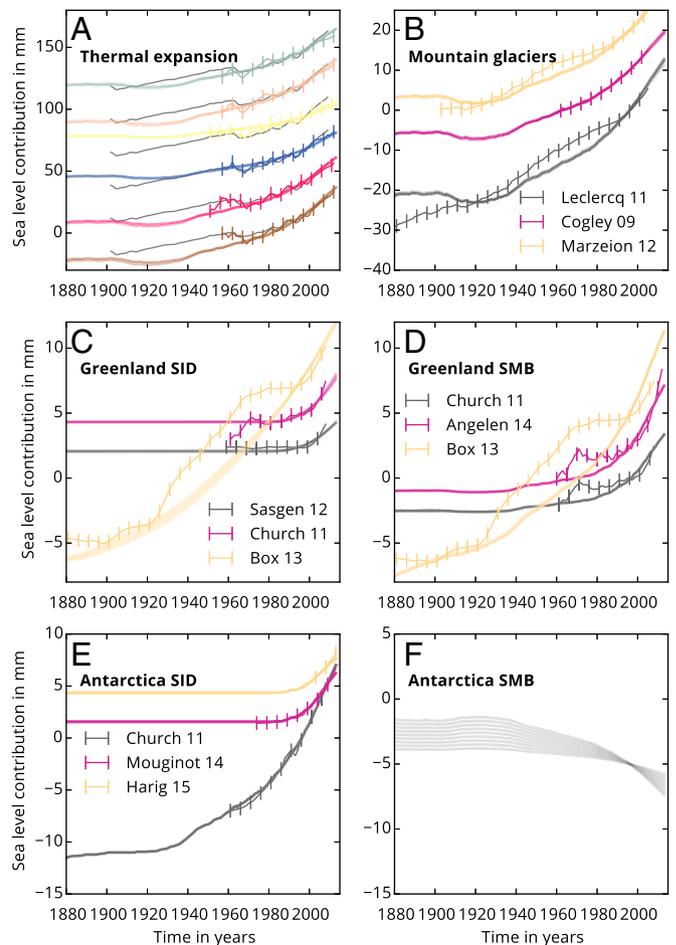

Fig. 1. Observed and calibrated sea level contributions. Observed (lines with bars) and calibrated sea level contribution (lines) during the calibration period for each sea level component. (*A*) Combinations of upper, middle, and deep ocean thermal expansion (12–15); only subset of all combinations shown; see Fig. S2 for full set. Gray lines show CMIP5 model mean (1). (*B*) Anthropogenic mountain glacier loss (18–20). (*C*) Greenland SID (26–28). (*D*) Greenland SMB (24–26). (*E*) Antarctic SID (26, 39, 40). The Antarctic SMB contribution (*F*) is not calibrated, and is provided here for comparison. All observations and calibrated contributions are relative to the 1986–2005 mean. An offset is applied between datasets for better visibility. The y axis scale varies between panels.

Greenland Surface Mass Balance. We use three different datasets for surface mass balance (SMB) reconstructions (24–26) of the Greenland ice sheet (see *Supporting Information* for details). The calibrated response time τ for the three observational datasets range from 99 y to 927 y, depending on the parameter α. The refs. 24 and 25 time series are well reproduced. For the ref. 24 time series, a preindustrial offset temperature needs to be applied (see *Supporting Information*). The recently observed high mass losses (25) are not fully captured by our global mean temperature-driven model.

The median future sea level contribution in 2100 from the Greenland ice sheet SMB is projected to be 7 cm, 12 cm, and 27 cm for the RCP26, RCP45, and RCP85 scenarios, respectively, relative to the 1986–2005 mean (Fig. 2*D*). Our projected 2081–2100 mean sea level is higher than ref. 3 estimates (Fig. 2*D*, bars at the right), with overlapping uncertainty ranges. The scenario dependency is also larger than estimated by IPCC, which is partly due to the assumed quadratic form of the millennial Greenland SMB sensitivity (see Eq. **3**).

Greenland Solid Ice Discharge. We use three observational datasets of past Greenland SID (26–28) to constrain our model (see

Fig. 2. Projected contributions to 21st century sea level rise for thermal expansion (*A*), mountain glaciers (*B*), Greenland solid ice discharge (*C*) and surface mass balance (*D*), and Antarctic solid ice discharge (*E*) and surface mass balance (*F*). Median (thick line) and fifth to 95th percentile uncertainty range (shading) of projected single contributions for the three RCP scenarios; based on 10,000 individual sea level curves. Bars at the right show fifth to 95th percentile range of this study (M16) and the IPCC AR5 (3) likely ranges intersected by the median for the 2081–2100 time mean. All are relative to the 1986–2005 mean. The *y* axis scale varies between panels.

Supporting Information for details). Because no long-term estimates are available for this contribution, we use a modified approach based on a response function driven by global mean temperature (see Eq. **4**). Although North Atlantic climate variability influences SID through oceanic and atmospheric drivers (29), a link between global warming and the speedup of Greenland's glaciers is plausible (30–32) and assumed valid within our model. The response is consistent with the observed range (Fig. 1*C*).

The projected global warming-driven ice dynamical contribution from Greenland (Fig. 2*C*) is small compared with the surface melting component. We estimate a stronger scenario dependency than the IPCC Fifth Assessment Report (AR5, ref. 3), with the RCP26 median being similar to IPCC, whereas the RCP45 and RCP85 medians exceed the respective IPCC AR5 2081–2100 mean. Even for the highest emission scenario, the median estimate for 2100 does not surpass 8 cm (see Table 1).

Antarctic Surface Mass Balance. The recent mass changes of the Antarctic ice sheet are predominantly of dynamic origin, with SMB not showing a significant trend (33, 34). We can therefore not calibrate the Antarctic SMB component with past global mean temperatures as a driver. However, the relation between Antarctic atmospheric warming and SMB is robustly linked through the temperature dependence of the water

carrying capacity of the atmosphere (35, 36) (see *Materials and Methods* for details).

Although we currently cannot model the Antarctic SMB with the pursuit curve method, we include the projected contribution in the total projections so that we are able to approximate total future anthropogenic sea level rise. The projection yields between 1.6 cm and 2.9 cm sea level drop during the 21st century, depending on the emission scenario (Fig. 2*F*), which is of a lower magnitude than the estimates of ref. 37 and the IPCC AR5 (3) due to the additional discharge effect reported in ref. 38.

Antarctic Solid Ice Discharge. Because the SMB of the ice sheet has not shown a significant trend in the past (33, 34), we assume total mass changes to be a proxy for the changes in SID. We use three observational datasets for Antarctic mass loss (26, 39, 40). We find similar response times for the refs. 40 and 26 datasets and slightly shorter response times for the ref. 39 dataset. All range from 1,350 y to 2,900 y. The calibrated sea level function reproduces the observed trend well (Fig. 1*E*) in all three cases.

Although the 20th century contribution of Antarctic SID is limited, projections for the 21st century yield a median contribution of 6 cm, 9 cm, and 13 cm for RCP26, RCP45, and RCP85 in the year 2100 (Fig. 2*E*). By construction, the contribution is scenario-dependent. Our RCP26 and RCP45 median estimates are similar to the scenario-independent IPCC AR5 values. The RCP85 median exceeds the IPCC median (Fig. 2*E*, bars at the right) but is consistent with post-IPCC-AR5 multimodel estimates (41). Our 90% uncertainty ranges for the three scenarios are enclosed in the uncertainty range provided by the IPCC.

Total Sea Level Rise. Comparing past observed total sea level rise to the sum of our calibrated contributions is an independent test for the validity of the method. We constructed the observed anthropogenic sea level curve by subtracting the nonanthropogenic glacier part (23) from the observations of total sea level rise of refs.

Fig. 3. Reconstructed and observed total anthropogenic sea level rise 1900 to today. Reconstructed sea level rise since 1900 as the sum of the probabilistically combined single contributions (median as brown line and 90% uncertainty range as shading) and observed sea level (blue, ref. 2; black, ref. 1; respective uncertainty ranges as shading). Only the anthropogenic part of the observed sea level is shown, produced by subtraction of the nonanthropogenic glacier contribution (23). All time series are relative to the 1986–2005 mean.

ENVIRONMENTAL SCIENCES

SUSTAINABILITY SCIENCE

Table 1. Twenty-first century anthropogenic sea level rise for single contributions and their sum

Contribution	RCP26	RCP45	RCP85
Thermal expansion	149.0 (66.2–228.0)	194.0 (85.8–303.0)	291.0 (120.0–454.0)
Mountain glaciers	79.0 (62.4–103.0)	93.2 (72.5–122.0)	109.0 (84.8–147.0)
Greenland SID	47.4 (35.1–87.2)	55.7 (41.5–109.0)	74.1 (50.8–147.0)
Greenland SMB	69.7 (40.1–116.0)	117.0 (69.3–214.0)	266.0 (152.0–518.0)
Antarctica SID	64.4 (40.4–91.0)	85.4 (55.9–124.0)	128.0 (88.8–189.0)
Antarctica SMB	−16.0 (−26.3 to −7.9)	−20.3 (−33.7 to −9.96)	−28.6 (−48.3 to −13.8)
Total	393.8 (279.9–555.5)	529.0 (370.8–772.7)	845.5 (574.1–1312.0)

Median, fifth percentile, and 95th percentile sea level rise for the year 2100 as anomaly to the reference period 1986–2005 in millimeters for the three RCP scenarios. See also Figs. 2 and 4 and Table S2.

1 and 2 (Fig. 3, black and blue lines). We produce a set of plausible past sea level curves by Monte Carlo sampling from the different observational datasets for the contributions and their respective tuples of commitment parameter and calibrated parameter (median as brown line in Fig. 3). Our estimate covers the past total sea level rise of ref. 2 since the 1940s. Early sea level rise is underestimated in comparison with both total sea level datasets, with the gap to the newer (2) data being smaller. Apart from glaciers and ice caps, other sea level contributors were likely not fully in equilibrium before the 20th century, so that they contributed to an early nonanthropogenic trend that is not captured by our method. This is probable for the inertial ice sheets that may still be responding to earlier forcing from the Holocene. Note that the observed total sea level rise has not been used for the calibration.

We project total anthropogenic sea level rise of 39 cm, 53 cm, and 85 cm until 2100 in the median for the RCP26, RCP45, and RCP85 scenarios, respectively, compared with the 1986–2005 mean (Table 1 and Fig. 4). Sea level rise does not exceed 131 cm within the 90% probability interval around the median of the high emission RCP85 scenario for 2100. Our estimates are consistent with the IPCC AR5 ranges, with a slightly higher scenario spread (Fig. 4, bars at the right, and Table S2 for 2081–2100 mean values). Note that the IPCC estimate includes land water storage and the uncertainty intervals represent likely ranges (66th percentile) and not very likely ranges (90th percentile).

Discussion and Conclusions

We assess future anthropogenic sea level rise based on calibrated relations between global mean temperature and each of the main sea level contributors. The method is fast, transparent, and consistent with the long-term commitment of the individual sea level contributions. Our contribution-based semiempirical approach aims to overcome the shortcomings of earlier semiempirical models while making use of their straightforward methodology. By design, the approach accounts for the available information for each sea level contributor, including the long-term commitment, possible saturation, and a specific response timescale. Classical semiempirical models fall short in incorporating such contribution-based information.

When calibrated against the individual contributions of observed sea level rise, our model reproduces the total sea level rise of the second half of the 20th century. Our reconstructed sea level rise in the beginning of the 20th century rise is lower compared with total sea level reconstructions (1, 2). This indicates the imperfect attribution of glacier losses due to early Arctic warming (22) and that longer-term nonanthropogenic trends may also be apparent in sea level contributors other than glaciers. Future research may resolve this gap by separating past natural and anthropogenic sources as has been done for glaciers (23). As our model is designed to only reproduce anthropogenic sea level rise, the early 20th century gap does not question the validity of the presented anthropogenic sea level projections. It highlights that contributions that cannot be easily linked to global mean temperature change may have played a significant role for early 20th century sea level rise. For thermal expansion, we assume a zero nonanthropogenic trend, although such trend cannot be fully ruled out because model simulations do not cover the time of the small ice age. There is, however, some evidence that the recent trend is largely anthropogenic (42, 43), which supports our assumption.

Long-term sensitivities to global mean temperature are only available for the following four components: thermal expansion, mountain glaciers, Greenland SMB, and Antarctic SID. These are the dominant contributors to past and future sea level rise and are treated consistently with the pursuit curve method. Greenland SID and Antarctic SMB are projected with a different method. Both components only play a minor role for 21st century sea level rise. For the Antarctic SMB, the simple scaling with surface temperature has been shown to be robust in a number of studies (36, 37).

The projected future sea level rise for RCP45 and RCP85 is not significantly higher than IPCC AR5 estimates, as opposed to most other semiempirical approaches. The projections show a larger scenario spread, mainly due to the high sensitivity of Greenland SMB projections. The newest SMB estimates of ref.
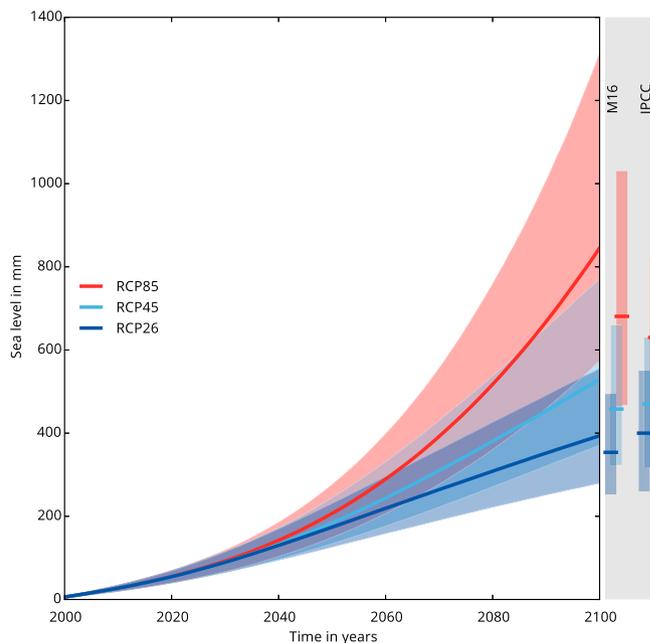

Fig. 4. Projected total anthropogenic sea level rise for the 21st century. Median (thick line) and fifth to 95th percentile uncertainty range (shading) of projected total anthropogenic sea level rise for three RCP scenarios as the sum of the single projected contributions (Fig. 2). Bars at the right show fifth to 95th percentile range of this study (M16) and the IPCC AR5 (3) likely ranges intersected by the median for 2081–2100. All are relative to the 1986–2005 mean.

25 show new records of surface melt on Greenland for recent years. These records are underestimated and therefore not fully linked to global mean temperature by our calibration (Fig. 1D), which is consistent with the suggested influence of natural variability through the North Atlantic oscillation (25, 44). Still, the inferred short response times lead to a future contribution above the range of current process-based projections (3). This highlights the importance of the attribution of recent melt records to anthropogenic forcing and raises the question of whether latest process-based estimates fully cover the mechanisms that drive 21st century Greenland surface mass loss.

As with other semiempirical approaches, our method cannot cover processes that are (or will become) independent of the forcing. Examples are the collapse of the Amundsen sector of the West Antarctic ice sheet, which is hypothesized to be already underway (45, 46), or a destabilization of the Wilkes basin in East Antarctica (47). The method can, however, account for processes that are not yet initiated but are reflected in the long-term sensitivity, which is an advantage over other semiempirical approaches. Contributions like groundwater depletion that are not linked to global warming (48) are not included in our calibration and do not bias our results. The model can be updated per contribution upon new physical insight, as, for example, for the dynamic discharge of the ice sheets. The method is limited to sea level contributors with monotonic long-term sensitivities. The Antarctic SMB may violate this condition for warming that is strong enough to initiate large-scale surface melting. Such melting is estimated to be small within this century (37) but may significantly reduce the ice body under strong greenhouse gas forcing in the long term (49).

The presented approach complements but cannot replace process-based modeling. It bridges the gap between classical semiempirical models and process-based models, because the parameters are chosen so that the model behavior is consistent with both past observations, which is a feature of semiempirical models, and long-term sensitivities as derived from process-based simulations. As opposed to complex process-based models, our method has low computational cost and can be used probabilistically. This allows the method to be incorporated in probabilistic impact studies that assess the causal chain of global warming from anthropogenic greenhouse gas emissions to the impacts of climate change.

Materials and Methods

Sea level rise in the 21st century is the combined response of highly inert systems to a common forcing. Therefore, it is reasonable to assume that the near-future response can be extrapolated from the past contributions, assuming the historical relationship between global mean warming and individual contributions remains the same. We use a pursuit curve to estimate the near-future sea level rise for each component as shown in Eq. 1. The applied long-term sensitivities S_{eq} are detailed below for each contribution.

Thermal expansion long-term sensitivity $S_{eq,te}$ can be inferred from long-term integrations of Earth system models of ntermediate complexity and be approximated as

$$S_{eq,te} = \alpha_{te} \cdot \Delta T \qquad [2]$$

with the commitment factor α_{te} and the deviation from preindustrial global mean temperature ΔT (5). Our estimates of α_{te} are based on six of such models and range from 0.2 m to 0.63 m per degree of warming (see *Supporting Information* for details).

For mountain glaciers, we apply a set of distinct functions $S_{eq,gic,i}$. Two different models (20, 50) have been used to estimate the glacier equilibrium sea level sensitivity globally (5). Forced by atmospheric data from 4 and 15 different climate models, respectively, they provide 19 different sensitivity curves for six levels of global warming, as shown in Fig. S4. As we are only interested in the ice loss that can be attributed to anthropogenic climate change, we remove the fraction caused by natural variability from the observational datasets and from the equilibrium sensitivities based on the data of ref. 23 (see *Supporting Information* for details).

The Greenland ice sheet is subject to an SMB feedback that leads to thresholds in the equilibrium response of total ice volume with respect to the surface air temperatures (51, 52). For sea level projections on centennial timescales, we rate the millennial (but not equilibrium) sensitivity to be a better approximation, as derived from refs. 5 and 52 and roughly of the form

$$S_{eq,gis,smb} = \alpha_{gis,smb} \cdot \Delta T^2 \qquad [3]$$

where $\alpha_{gis,smb}$ ranges from 0.05 to 0.21 m °C^{-2} and ΔT denotes the global mean temperature anomaly above preindustrial.

An estimate of the long-term sensitivity of Greenland's SID to global warming is not available. We thus modify the approach for this contribution following ref. 53. In response to ocean warming, the mechanical frontal stress at the marine termini of outlet glaciers is reduced, leading to enhanced ice discharge from Greenland (53). Increased melt water through a warmer atmosphere can lead to increased lubrication that speeds up glaciers and increases discharge (30–32). We here assume that frontal stress release (54) and runoff lubrication (27) can be approximated as linearly depending the global mean temperature anomaly ΔT. Ref. 55 has shown that the resulting sea level rise from Greenland's dynamic discharge $S_{gis,dyn}$ can be described via the response function

$$\frac{dS_{gis,dyn}}{dt}(t) = \Gamma \int_0^t \left(\frac{t-t'}{t_0} \right)^\beta \Delta T dt' \qquad [4]$$

with β equal to -0.7 and temperature anomaly ΔT. We estimate the prefactor Γ in the interval 1.6–11×10^{-5} m·y^{-2}·K^{-1}. This factor implies that a linear scaling between the global mean temperature and the local temperatures is applicable. To cover the uncertainty in the response, we here vary β between -0.9 to -0.5; t_0 is only used to nondimensionalize the time dependence and is chosen as 1 y.

In Antarctica, the observed relation between temperature and snowfall increase has been shown to be almost linear on centennial timescales. Ref. 37 estimated the sea level sensitivity to Antarctic warming to be 2.7 mm·y^{-1} per degree Celsius. Other studies found different scaling factors (see ref. 36 and table 4 in ref. 37), and, to reflect these, we vary the factor between 2 mm·y^{-1} per degree Celsius and 5 mm·y^{-1} per degree Celsius.

We do not apply a scaling factor between global and Antarctic atmospheric temperature change because the polar amplification is negligible for Antarctica (56). Ref. 38 showed that the increase in snowfall and the consequent steepening of the surface gradient at the grounding line leads to enhanced dynamic discharge along the coastline of Antarctica, which compensates between 15% and 35% of the mass gain through snowfall on a centennial timescale.

The SMB change from Antarctica is therefore estimated via

$$\frac{dS_{ais,smb}}{dt}(t) = -(1-\kappa) \cdot \gamma \cdot \Delta T \qquad [5]$$

where ΔT denotes the global mean temperature change, γ is the snowfall sensitivity, and κ is the fraction lost due to the increase in dynamic discharge. We use a constant κ of 0.25 within this study.

Quasi-equilibrium estimates for the Antarctic ice sheet dynamic discharge contribution to sea level rise have been derived in ref. 5 from a 5-million-year simulation of the Antarctic ice sheet (57). A relatively constant commitment of $\alpha_{ais,dyn}$ 1.2 m sea level per degree of warming is deduced from correlating global mean temperature with ice volume (figure 1D in ref. 5),

$$S_{eq,ais,dyn} = \alpha_{ais,dyn} \cdot \Delta T \qquad [6]$$

We account for the uncertainty that originates from forcing data, ice physics, and memory of the ice sheet by sampling α from the interval [1.0–1.5] m per degree Celsius, which reflects the first standard deviation of the model simulations on which the relation is based.

For all contributions, we apply Monte Carlo sampling to project future sea level rise including observational and climate system uncertainties. Sea level uncertainty is covered by sampling from the calibrated set of semiempirical functions, which incorporates the various observations and long-term responses. The uncertainty in the climate system response to future greenhouse gas emissions is accounted for by sampling from an ensemble of 600 global mean temperature pathways for the three representative concentration pathways RCP26, RCP45, and RCP85 (17). The pathways, produced by the MAGICC 6.0 simple climate model (58), are consistent with past climate change and the results from climate models of higher complexity (59). To capture sea level and climatic uncertainty, we repeat the procedure 10,000 times. Uncertainty intervals are calculated on the basis of the 10,000 sea level curves.

ENVIRONMENTAL SCIENCES

SUSTAINABILITY SCIENCE

1. Church JA, White NJ (2011) Sea-level rise from the late 19th to the early 21st century. *Surv Geophys* 32(4):585–602.
2. Hay CC, Morrow E, Kopp RE, Mitrovica JX (2015) Probabilistic reanalysis of twentieth-century sea-level rise. *Nature* 517(7535):481–484.
3. Intergovernmental Panel on Climate Change (2014) *Climate Change 2013 - The Physical Science Basis: Working Group I Contribution to the Fifth Assessment Report of the Intergovernmental Panel on Climate Change* (Cambridge Univ Press, New York).
4. Masters D, et al. (2012) Comparison of global mean sea level time series from TOPEX/Poseidon, Jason-1, and Jason-2. *Mar Geod* 35(Suppl 1):20–41.
5. Levermann A, et al. (2013) The multimillennial sea-level commitment of global warming. *Proc Natl Acad Sci USA* 110(34):13745–13750.
6. Intergovernmental Panel on Climate Change (2014) *Climate Change 2013 - Impacts, Adaptation, and Vulnerability Working Group II Contribution to the Fifth Assessment Report of the Intergovernmental Panel on Climate Change* (Cambridge Univ Press, New York).
7. Rahmstorf S (2007) A semi-empirical approach to projecting future sea-level rise. *Science* 315(5810):368–370.
8. Vermeer M, Rahmstorf S (2009) Global sea level linked to global temperature. *Proc Natl Acad Sci USA* 106(51):21527–21532.
9. Jevrejeva S, Moore JC, Grinsted A (2010) How will sea level respond to changes in natural and anthropogenic forcings by 2100? *Geophys Res Lett* 37(7):L07703.
10. Grinsted A, Moore JC, Jevrejeva S (2010) Reconstructing sea level from paleo and projected temperatures 200 to 2100 AD. *Clim Dyn* 34(4):461–472.
11. Dutton A, et al. (2015) Sea-level rise due to polar ice-sheet mass loss during past warm periods. *Science* 349(6244):aaa4019.
12. Domingues CM, et al. (2008) Improved estimates of upper-ocean warming and multi-decadal sea-level rise. *Nature* 453(7198):1090–1093.
13. Ishii M, Kimoto M (2009) Reevaluation of historical ocean heat content variations with time-varying XBT and MBT depth bias corrections. *J Oceanogr* 65(3):287–299.
14. Levitus S, et al. (2012) World ocean heat content and thermosteric sea level change (0–2000 m), 1955–2010. *Geophys Res Lett* 39(10):L10603.
15. Purkey SG, Johnson GC (2010) Warming of global abyssal and deep southern ocean waters between the 1990s and 2000s: Contributions to global heat and sea level rise budgets. *J Clim* 23(23):6336–6351.
16. Hansen JE, Ruedy R, Sato M, Lo K (2009) *NASA GISS Surface Temperature (GISTEMP) Analysis*. Available at cdiac.ornl.gov/trends/temp/hansen/hansen.html. Accessed December, 2014.
17. van Vuuren DP, et al. (2011) The representative concentration pathways: An overview. *Clim Change* 109(1-2):5–31.
18. Cogley JG (2009) Geodetic and direct mass-balance measurements: Comparison and joint analysis. *Ann Glaciol* 50:96–100.
19. Leclercq PW, Oerlemans J, Cogley JG (2011) Estimating the glacier contribution to sea-level rise for the period 1800–2005. *Surv Geophys* 32(4-5):519–535.
20. Marzeion B, Jarosch AH, Hofer M (2012) Past and future sea-level change from the surface mass balance of glaciers. *Cryosphere* 6:1295–1322.
21. Marzeion B, Leclercq PW, Cogley JG, Jarosch AH (2015) Brief Communication: Global reconstructions of glacier mass change during the 20th century are consistent. *Cryosphere* 9:2399–2404.
22. Fyfe JC, et al. (2013) One hundred years of Arctic surface temperature variation due to anthropogenic influence. *Sci Rep* 3:2645.
23. Marzeion B, Cogley JG, Richter K, Parkes D (2014) Glaciers. Attribution of global glacier mass loss to anthropogenic and natural causes. *Science* 345(6199):919–921.
24. Box JE (2013) Greenland Ice Sheet mass balance reconstruction. Part II: Surface mass balance (1840–2010). *J Clim* 26(18):6974–6989.
25. van Angelen JH, van den Broeke MR, Wouters B, Lenaerts JTM (2014) Contemporary (1960–2012) evolution of the climate and surface mass balance of the Greenland Ice Sheet. *Surv Geophys* 35(5):1155–1174.
26. Church JA, et al. (2011) Revisiting the Earth's sea-level and energy budgets from 1961 to 2008. *Geophys Res Lett* 38(18):L18601.
27. Box JE, Colgan W (2013) Greenland Ice Sheet mass balance reconstruction. Part III: Marine ice loss and total mass balance (1840–2010). *J Clim* 26(18):6990–7002.
28. Sasgen I, et al. (2012) Timing and origin of recent regional ice-mass loss in Greenland. *Earth Planet Sci Lett* 333-334:293–303.
29. Straneo F, et al. (2013) Challenges to understanding the dynamic response of Greenland's marine terminating glaciers to oceanic and atmospheric forcing. *Bull Am Meteorol Soc* 94(8):1131–1144.
30. Zwally HJ, et al. (2002) Surface melt-induced acceleration of Greenland ice-sheet flow. *Science* 297(5579):218–222.
31. van de Wal RSW, et al. (2008) Large and rapid melt-induced velocity changes in the ablation zone of the Greenland Ice Sheet. *Science* 321(5885):111–113.
32. Doyle SH, et al. (2015) Amplified melt and flow of the Greenland ice sheet driven by late-summer cyclonic rainfall. *Nat Geosci* 8(8):647–653.
33. Monaghan AJ, et al. (2006) Insignificant change in Antarctic snowfall since the International Geophysical Year. *Science* 313(5788):827–831.
34. Lenaerts JTM, van den Broeke MR, van de Berg WJ, van Meijgaard E, Kuipers Munneke P (2012) A new, high-resolution surface mass balance map of Antarctica (1979–2010) based on regional atmospheric climate modeling. *Geophys Res Lett* 39(4):L04501.
35. Held IM, Soden BJ (2006) Robust responses of the hydrological cycle to global warming. *J Clim* 19(21):5686–5699.
36. Frieler K, et al. (2015) Consistent evidence of increasing Antarctic accumulation with warming. *Nat Clim Chang* 5(4):348–352.
37. Ligtenberg SRM, van de Berg WJ, van den Broeke MR, Rae JGL, van Meijgaard E (2013) Future surface mass balance of the Antarctic ice sheet and its influence on sea level change, simulated by a regional atmospheric climate model. *Clim Dyn* 41(3):867–884.
38. Winkelmann R, Levermann A, Martin MA, Frieler K (2012) Increased future ice discharge from Antarctica owing to higher snowfall. *Nature* 492(7428):239–242.
39. Mouginot J, Rignot E, Scheuchl B (2014) Sustained increase in ice discharge from the Amundsen Sea Embayment, West Antarctica, from 1973 to 2013. *Geophys Res Lett* 41(5):1576–1584.
40. Harig C, Simons FJ (2015) Accelerated West Antarctic ice mass loss continues to outpace East Antarctic gains. *Earth Planet Sci Lett* 415:134–141.
41. Levermann A, et al. (2014) Projecting Antarctic ice discharge using response functions from SeaRISE ice-sheet models. *Earth Syst. Dyn.* 5(2):271–293.
42. Hobbs WR, Willis JK (2013) Detection of an observed 135 year ocean temperature change from limited data. *Geophys Res Lett* 40(10):2252–2258.
43. Slangen ABA, Church JA, Zhang X, Monselesan D (2014) Detection and attribution of global mean thermosteric sea level change. *Geophys Res Lett* 41(16):5951–5959.
44. Hanna E, et al. (2014) Atmospheric and oceanic climate forcing of the exceptional Greenland ice sheet surface melt in summer 2012. *Int J Climatol* 34(4):1022–1037.
45. Favier L, et al. (2014) Retreat of Pine Island Glacier controlled by marine ice-sheet instability. *Nat Clim Chang* 4:117–121.
46. Joughin I, Smith BE, Medley B (2014) Marine ice sheet collapse potentially under way for the Thwaites Glacier Basin, West Antarctica. *Science* 344(6185):735–738.
47. Mengel M, Levermann A (2014) Ice plug prevents irreversible discharge from East Antarctica. *Nat Clim Chang* 4:451–455.
48. Orlić M, Pasarić Z (2013) Semi-empirical versus process-based sea-level projections for the twenty-first century. *Nat Clim Chang* 3:735–738.
49. Winkelmann R, Levermann A, Ridgwell A, Caldeira K (2015) Combustion of available fossil fuel resources sufficient to eliminate the Antarctic Ice Sheet. *Sci Adv* 1(8):e1500589.
50. Radić V, Hock R (2010) Regional and global volumes of glaciers derived from statistical upscaling of glacier inventory data. *J Geophys Res* 115(F1):F01010.
51. Ridley J, Gregory JM, Huybrechts P, Lowe J (2010) Thresholds for irreversible decline of the Greenland ice sheet. *Clim Dyn* 35(6):1049–1057.
52. Robinson A, Calov R, Ganopolski A (2012) Multistability and critical thresholds of the Greenland ice sheet. *Nat Clim Chang* 2:429–432.
53. Price SF, Payne AJ, Howat IM, Smith BE (2011) Committed sea-level rise for the next century from Greenland ice sheet dynamics during the past decade. *Proc Natl Acad Sci USA* 108(22):8978–8983.
54. Luckman A, et al. (2015) Calving rates at tidewater glaciers vary strongly with ocean temperature. *Nat Commun* 6:8566.
55. Winkelmann R, Levermann A (2013) Linear response functions to project contributions to future sea level. *Clim Dyn* 40(11):2579–2588.
56. Frieler K, Meinshausen M, Mengel M, Braun N, Hare W (2012) A scaling approach to probabilistic assessment of regional climate change. *J Clim* 25(9):3117–3144.
57. Pollard D, DeConto RM (2009) Modelling West Antarctic ice sheet growth and collapse through the past five million years. *Nature* 458(7236):329–332.
58. Meinshausen M, Raper SCB, Wigley TML (2011) Emulating coupled atmosphere-ocean and carbon cycle models with a simpler model, MAGICC6 – Part 1: Model description and calibration. *Atmos Chem Phys* 11(4):1417–1456.
59. Meinshausen M, et al. (2009) Greenhouse-gas emission targets for limiting global warming to 2 °C. *Nature* 458(7242):1158–1162.
60. Abraham JP, et al. (2013) A review of global ocean temperature observations: Implications for ocean heat content estimates and climate change. *Rev Geophys* 51(3):450–483.
61. Llovel W, Willis JK, Landerer FW, Fukumori I (2014) Deep-ocean contribution to sea level and energy budget not detectable over the past decade. *Nat Clim Chang* 4:1031–1035.
62. Intergovernmental Panel on Climate Change (2007) *Climate Change 2007: The Physical Science Basis. Contribution of Working Group I to the Fourth Assessment Report of the Intergovernmental Panel on Climate Change* (Cambridge Univ Press, New York).
63. New M, Lister D, Hulme M, Makin I (2002) A high-resolution data set of surface climate over global land areas. *Clim Res* 21:1–25.
64. Mitchell TD, Jones PD (2005) An improved method of constructing a database of monthly climate observations and associated high-resolution grids. *Int J Climatol* 25(6):693–712.
65. Pfeffer WT, et al. (2014) The Randolph Glacier Inventory: A globally complete inventory of glaciers. *J Glaciol* 60(221):537–552.
66. Rignot E, Box JE, Burgess E, Hanna E (2008) Mass balance of the Greenland ice sheet from 1958 to 2007. *Geophys Res Lett* 35(20):L20502.
67. Hanna E, et al. (2011) Greenland Ice Sheet surface mass balance 1870 to 2010 based on Twentieth Century Reanalysis, and links with global climate forcing. *J Geophys Res* 116(D24):D24121.
68. Wahr J, Swenson S, Velicogna I (2006) Accuracy of GRACE mass estimates. *Geophys Res Lett* 33(6):L06401.
69. Enderlin EM, et al. (2014) An improved mass budget for the Greenland ice sheet. *Geophys Res Lett* 41(3):866–872.
70. Csatho BM, et al. (2014) Laser altimetry reveals complex pattern of Greenland Ice Sheet dynamics. *Proc Natl Acad Sci USA* 111(52):18478–18483.
71. van den Broeke M, et al. (2009) Partitioning recent Greenland mass loss. *Science* 326(5955):984–986.
72. Rignot E, Velicogna I, van den Broeke MR, Monaghan A, Lenaerts JTM (2011) Acceleration of the contribution of the Greenland and Antarctic ice sheets to sea level rise. *Geophys Res Lett* 38(5):L05503.
73. Rignot E (2008) Changes in West Antarctic ice stream dynamics observed with ALOS PALSAR data. *Geophys Res Lett* 35(12):L12505.